Utility Workspace of 3-5R Translational Parallel Mechanism

Masataka Tanabe
Department of Mechanical Sciences and Engineering
Tokyo Institute of Technology
Tokyo, Japan

Syamsul Huda
Department of Mechanical Sciences and Engineering
Tokyo Institute of Technology
Tokyo, Japan

Yukio Takeda
Department of Mechanical Sciences and Engineering
Tokyo Institute of Technology
Tokyo, Japan
takeda@mech.titech.ac.jp

***Abstract*— In the present paper, we discussed about a kinamatic design of 3-5R translational parallel mechanism with a large utility workspace. We defined the utility workspace as a closed area, from any point to other points in which the mechanism can move without suffering from singularity and workspace boundary. A computational algorithm of the volume of the utility workspace was proposed. We discussed about the utility workspace of 3-5R translational parallel mechanisms having three types of chain with consideration of actuation and constraint singularities. We obtained a 3-RUU translational parallel mechanism with a large utility workspace.**

***Keywords*— Robotics, Kinematic design, Translational parallel mechanism, Utility workspace, Singularity**

I. Introduction

A parallel mechanism which has three degrees of freedom and performs pure translational output motion without changing its orientation is called a “translational parallel mechanism”. A translational parallel mechanism has potential applications in pick and place, machining, coordinate measurement, and so on. A translational parallel mechanism is composed of a base, a platform and multiple connecting chains arranged in parallel between the base and platform.

In recent years, many researchers have interests in translational parallel mechanisms and manipulators. Kinematic condition of the connecting chain to obtain pure translational motion of the platform has been investigated in [3]-[5]. Various kinematic structures of translational parallel mechanism, 3-URC type [8], 3-PRRR type [9][19][20], and 3-UPU type [10], etc., have been investigated. Here, C, P, R and U represent cylindrical, prismatic, revolute and universal joints, respectively. Mechanisms with a connecting chain that constrains rotational motion of the platform and does not have any active joint, called supporting leg, have been proposed in [6][7]. Workspace of 3-5R parallel mechanism has been investigated in [2]. Optimization of the mechanism considering its workspace using the global conditioning index has been done in [11]-[14]. Translational parallel mechanisms have been applied to a chest compression machine in the process of cardiopulmonary resuscitation [15] and micro manipulators [16][17]. Singularity of lower-dof parallel mechanism has been investigated in [22]-[24].

Even though there are applications of translational parallel mechanism as described above, there exist many problems in its design. One of the problems is the division of reachable workspace into some independent sub-workspaces due to the existence of singular points because the area in which mechanism can actually work is limited within a consecutive area which does not include singularity. Once the mechanism is assembled, it can move inside a sub-workspace that is surrounded by singularity surfaces and workspace boundaries. The largest area among the sub-workspaces is called “utility workspace” in the present paper. Key issue of the mechanism design is to obtain a mechanism with a larger utility workspace by optimizing its structure and its dimensions.

In the last two decades, singular points of parallel mechanisms with six degrees of freedom have been extensively investigated, and many works related to mechanism design with consideration of utility workspace have been done. For the parallel mechanism with six degrees of freedom, actuation singularity (forward kinematic singularity) should be mainly considered. However, for lower-dof parallel mechanisms such as translational parallel mechanism, constraint singularity as well as actuation singularity should be simultaneously considered in their design.

In the present paper, we discuss about the kinematic design of translational parallel mechanism which has three connecting chains with five revolute joints with consideration of utility workspace taking actuation and constraint singularities into consideration. A technique to compute the volume of utility workspace from digitized data of the reachable workspace is also presented. Through numerical examples, we show a structure and dimensions of a translational parallel mechanism having a large utility workspace. Finally, a prototype is briefly introduced.

II. 3-5R Translational Spatial Parallel Mechanism

A. Mechanism Configuration

Figure 1 shows a 3-5R translational spatial parallel mechanism. It has three connecting chains, and they are symmetrically located between the platform and the base. Each connecting chain consists of five revolute joints. When three of the five revolute joints are parallel and resultant two are parallel in each connecting chain, the mechanism performs pure translational platform motion [5]. In the mechanism shown in Fig.1, the first, second and fifth revolute joints are parallel, and the third and fourth are parallel. This type of connecting chain is denoted as $\dot{R}\dot{R}\overline{RR}\dot{R}$ by using bar or dot on R to clearly indicate geometrical relationship among five joint axes. An $\dot{R}\dot{R}\overline{RR}\dot{R}$ chain constrains a rotational motion of the platform around an axis perpendicular to joint axes 1 and 3. Because there are three connecting chains, the platform's rotational motion is completely constrained as far as constraints by three connecting chains are independent.

B. Coordinate Systems

A coordinate system O-XYZ is attached on the base. The first revolute joint of each connecting chain is symmetrically located on a circle which is perpendicular to the Y-axis. A coordinate system $\mathrm{A}_i - x_i y_i z_i$ is located at A_i on the base as shown in Fig. 2, so that $x_i z_i$ plane is parallel to the XZ plane and z_i is the axis of rotation of the first revolute joint, where i denotes the connecting chain's number ($i = 1,2,3$).

C. Kinematic Constants and Variables

Following the definition of the D-H parameters, kinematic constants to describe the relationship between adjacent joints are defined as shown in Fig. 2(d). To describe the location of the revolute joints on the base and the platform, kinematic constants r_{b}, r_{p} and γ_i are used as shown in Figs. 2(b) and 2(c). In the present paper, $\gamma_1 = 0^\circ$, $\gamma_2 = 120^\circ$, $\gamma_3 = 240^\circ$, $\alpha_{12} = \alpha_{34} = 0, \alpha_{23} = \alpha_{45} = 90^\circ$ are commonly used unless specified.

Each revolute joint on the base is considered as active joint. Angular displacements of the active joints are denoted as $\boldsymbol{\theta} = [\theta_{1,1}\ \theta_{1,2}\ \theta_{1,3}]^{\mathrm{T}}$ as shown in Fig. 2(b). The direction of the j-th(j=1,2,…5) joint in the i-th connecting chain is denoted as $\boldsymbol{w}_{j,i}$, and the position of the j-th joint of the i-th connecting chain is denoted as $\boldsymbol{r}_{j,i}$.

III. Singularity Analysis

There exist four types of singularity in parallel mechanism. Two of them are actuation singularity and constraint singularity at which the mechanism cannot keep its configuration even when all actuators are locked. These types of singularity are seen only in closed-loop mechanism. The other two types of singularity are one that locates at the workspace boundary and the other at which one of the connecting chains has local mobility. In the design of parallel mechanism, the former two singularities should be carefully considered. In this section, a method to find constraint and actuation singularities of 3-5R parallel mechanism with $\dot{R}\dot{R}\overline{RR}\dot{R}$ connecting chains is described.

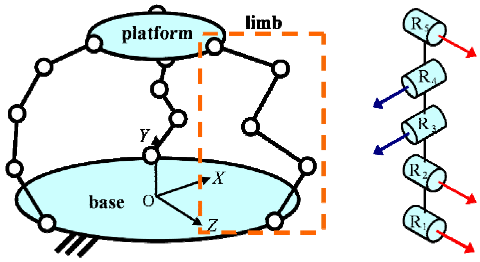

Figure 1. 3-5R translational spatial parallel mechanism having $\dot{R}\dot{R}\overline{RR}\dot{R}$ connecting chains

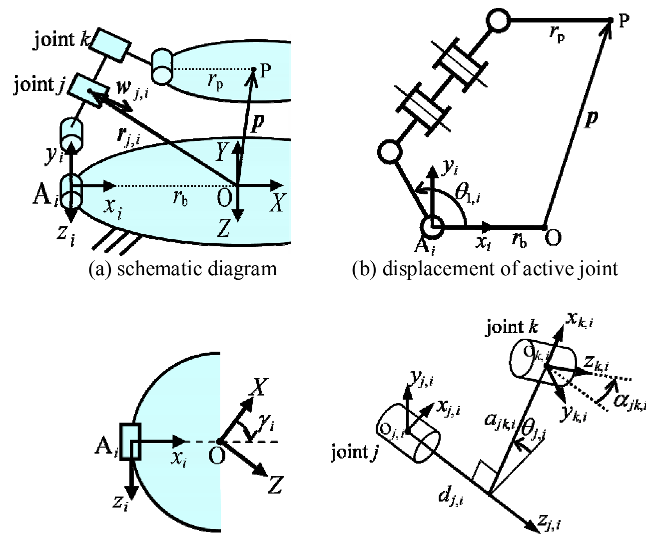

(a) schematic diagram (b) displacement of active joint

(c) location of a connecting chain (d) DH parameters

Figure 2. Coordinate systems and kinematic parameters

A. Velocity Relationship

Because 3-5R parallel mechanism is spatial parallel mechanism with three dof, constraint equation as well as input-output velocity relationship should be considered to investigate instantaneous characteristics of the mechanism. Using a 6×6 overall Jacobian matrix J_{T} defined in [1], the velocity relationship of the mechanism is described as

$$J_{\mathrm{T}} \begin{bmatrix} \boldsymbol{\omega} \\ \boldsymbol{v} \end{bmatrix} = \begin{bmatrix} \dot{\boldsymbol{\theta}} \\ \mathbf{0} \end{bmatrix}, \tag{1}$$

where $\boldsymbol{\omega}$ and $\boldsymbol{v}$ are angular velocity vector, translational velocity vector of the platform, and $\dot{\boldsymbol{\theta}}$ and $\mathbf{0}$ are input velocity vector and three dimensional zero vector, respectively. The upper three scalar equations of Eq. (1) describe the relationship between input and output velocities, and the lower the constraint equation. The overall Jacobian matrix can be written using 3×3 matrices J_{a}, J_{b} and J_{c} as

$$J_{\mathrm{T}} = \begin{bmatrix} J_{\mathrm{b}} & J_{\mathrm{a}} \\ J_{\mathrm{c}} & 0_3 \end{bmatrix}, \tag{2}$$

where 0_3 represents the three dimensional zero matrix. These matrices are derived in III.D.

B. Constraint Singularity

The constraint equation of 3-5R translational parallel mechanism is written as

$$J_{\mathrm{c}}\boldsymbol{\omega} = \mathbf{0}. \tag{3}$$

When the rank of the matrix J_{c} is less than three, constraint imposed on the platform by three connecting chains are dependent. Then, rotational motion of the platform can not be constrained. This is the constraint singularity. Therefore, the constraint singularity is defined by

$$\det J_{\mathrm{c}} = 0. \tag{4}$$

C. Actuation Singularity

If the rank of the matrix J_{c} is three, the mechanism can perform three-dof pure translational platform motion. In this situation, the following relationship between input and output velocities holds

$$J_{\mathrm{a}}\boldsymbol{v} = \dot{\boldsymbol{\theta}}. \tag{5}$$

When the rank of the matrix J_{a} is less than three, translational motion of the platform can not be constrained even if all the input joints are locked. This is the actuation singularity. Therefore, the actuation singularity is defined by

$$\det J_{\mathrm{a}} = 0. \tag{6}$$

D. Derivation of Matrices J_{a} and J_{c}

Firstly, the matrix J_{c} is derived using the reciprocal screw theory. Joint screw $\boldsymbol{S}_{j,i}$ (six dimensional vector) of the j-th joint in the i-th connecting chain is denoted as

$$\boldsymbol{S}_{j,i} = \begin{bmatrix} \boldsymbol{s}_{\mathrm{r},j,i}^{\mathrm{T}} & \boldsymbol{s}_{\mathrm{t},j,i}^{\mathrm{T}} \end{bmatrix}^{\mathrm{T}} = \begin{bmatrix} \boldsymbol{w}_{j,i}^{\mathrm{T}} & \left(\boldsymbol{r}_{j,i} \times \boldsymbol{w}_{j,i}\right)^{\mathrm{T}} \end{bmatrix}^{\mathrm{T}},$$

where $\boldsymbol{s}_{\mathrm{r},j,i}$ and $\boldsymbol{s}_{\mathrm{t},j,i}$ are three dimensional vectors. Consider a screw that is reciprocal to all joint screws of each connecting chain. Such a reciprocal screw is denoted as $\boldsymbol{S}_{\mathrm{R},i} = \begin{bmatrix} \boldsymbol{s}_{\mathrm{Rf},i}^{\mathrm{T}} & \boldsymbol{s}_{\mathrm{Rm},i}^{\mathrm{T}} \end{bmatrix}^{\mathrm{T}}$, where $\boldsymbol{s}_{\mathrm{Rf},i}$ and $\boldsymbol{s}_{\mathrm{Rm},i}$ are three dimensional vectors and represent constraint force and moment imposed on the platform by the i-th connecting chain. Since the virtual power by a constraint force by a connecting chain and velocity of the platform generated by each joint velocity of a connecting chain should be zero, $\boldsymbol{S}_{\mathrm{R},i}$ is obtained by solving the following equation,

$$\boldsymbol{S}_{\mathrm{R},i} \circ \boldsymbol{S}_{j,i} = \boldsymbol{s}_{\mathrm{Rf},i}^{\mathrm{T}}\boldsymbol{s}_{\mathrm{t},j,i} + \boldsymbol{s}_{\mathrm{Rm},i}^{\mathrm{T}}\boldsymbol{s}_{\mathrm{r},j,i} = 0 \, (j = 1, 2, \cdots, 5), \tag{7}$$

where the operator $\circ$ represents the reciprocal product.

The output velocity $\boldsymbol{V} = \begin{bmatrix} \boldsymbol{\omega}_{\mathrm{O}}^{\mathrm{T}} & \boldsymbol{v}_{\mathrm{O}}^{\mathrm{T}} \end{bmatrix}^{\mathrm{T}}$ is written as

$$\boldsymbol{V} = \sum_{j=1}^{5} \boldsymbol{S}_{j,i}\,\dot{\theta}_{j,i}. \tag{8}$$

Applying the reciprocal product with $\boldsymbol{S}_{\mathrm{R},i}$ to both sides of Eq. (8) and substituting the relationship in Eq. (7) into this equation, the following relationship is obtained.

$$\boldsymbol{S}_{\mathrm{R},i} \circ \boldsymbol{V} = 0 \tag{9}$$

Substituting the conditions where $\boldsymbol{w}_{1,i} = \boldsymbol{w}_{2,i} = \boldsymbol{w}_{5,i}$ and $\boldsymbol{w}_{3,i} = \boldsymbol{w}_{4,i}$ into Eq. (7), $\boldsymbol{S}_{\mathrm{R},i}$ for a 3-5R parallel mechanism with $\dot{\mathrm{R}}\dot{\mathrm{R}}\overline{\mathrm{RR}}\dot{\mathrm{R}}$ connecting chains is obtained as

$$\boldsymbol{s}_{\mathrm{Rf},i} = \mathbf{0}, \quad \boldsymbol{s}_{\mathrm{Rm},i} = \frac{\boldsymbol{w}_{1,i} \times \boldsymbol{w}_{3,i}}{\left|\boldsymbol{w}_{1,i} \times \boldsymbol{w}_{3,i}\right|}. \tag{10}$$

Using Eqs. (9) and (10), the matrix J_{c} is obtained as

$$J_c = \begin{bmatrix} \boldsymbol{s}_{\mathrm{Rm},1}^{\mathrm{T}} \\ \boldsymbol{s}_{\mathrm{Rm},2}^{\mathrm{T}} \\ \boldsymbol{s}_{\mathrm{Rm},3}^{\mathrm{T}} \end{bmatrix} = \begin{bmatrix} (\boldsymbol{w}_{1,1} \times \boldsymbol{w}_{3,1})^{\mathrm{T}} / \left|\boldsymbol{w}_{1,1} \times \boldsymbol{w}_{3,1}\right| \\ (\boldsymbol{w}_{1,2} \times \boldsymbol{w}_{3,2})^{\mathrm{T}} / \left|\boldsymbol{w}_{1,2} \times \boldsymbol{w}_{3,2}\right| \\ (\boldsymbol{w}_{1,3} \times \boldsymbol{w}_{3,3})^{\mathrm{T}} / \left|\boldsymbol{w}_{1,3} \times \boldsymbol{w}_{3,3}\right| \end{bmatrix}. \tag{11}$$

Next, the matrix J_{a} is derived. A screw $\boldsymbol{S}_{\mathrm{RA},i} = \begin{bmatrix} \boldsymbol{s}_{\mathrm{RAf},i}^{\mathrm{T}} & \boldsymbol{s}_{\mathrm{RAm},i}^{\mathrm{T}} \end{bmatrix}^{\mathrm{T}}$ which satisfies the following equations is considered.

$$\left.\begin{aligned} &\boldsymbol{S}_{\mathrm{RA},i} \circ \boldsymbol{S}_{k,i} = 0, \quad k = 2,3,4,5 \\ &\boldsymbol{S}_{\mathrm{RA},i} \bullet \boldsymbol{S}_{\mathrm{R},i} = 0 \end{aligned}\right\} \tag{12}$$

Here the operator $\bullet$ represents the inner product. For a 3-5R parallel mechanism with $\dot{\mathrm{R}}\dot{\mathrm{R}}\overline{\mathrm{RR}}\dot{\mathrm{R}}$ connecting chains, the screw is obtained as

$$\left.\begin{aligned} &\boldsymbol{s}_{\mathrm{RAf},i} = \left\{\left(\boldsymbol{r}_{2,i} - \boldsymbol{r}_{5,i}\right) \times \boldsymbol{w}_{1,i}\right\} \times \left\{\left(\boldsymbol{r}_{3,i} - \boldsymbol{r}_{4,i}\right) \times \boldsymbol{w}_{3,i}\right\} \\ &\boldsymbol{s}_{\mathrm{RAm},i} = m\boldsymbol{w}_{1,i} + n\boldsymbol{w}_{3,i} \end{aligned}\right\}, \tag{13}$$

where

$$m = \frac{(F - \boldsymbol{w}_{1,i} \bullet \boldsymbol{w}_{3,i} F')}{\left(\boldsymbol{w}_{1,i} \bullet \boldsymbol{w}_{3,i}\right)^2 - 1}, \quad n = \frac{(F' - \boldsymbol{w}_{1,i} \bullet \boldsymbol{w}_{3,i} F)}{\left(\boldsymbol{w}_{1,i} \bullet \boldsymbol{w}_{3,i}\right)^2 - 1}.$$

$$F = \boldsymbol{s}_{\mathrm{RAf},i} \bullet \left(\boldsymbol{r}_{2,i} \times \boldsymbol{w}_{1,i}\right), \quad F' = \boldsymbol{s}_{\mathrm{RAf},i} \bullet \left(\boldsymbol{r}_{3,i} \times \boldsymbol{w}_{3,i}\right)$$

Applying the reciprocal product with $\boldsymbol{S}_{\mathrm{RA},i}$ to both sides of Eq. (8) and substituting the relationship in Eq. (13) into this equation, the following relationship is obtained.

$$\boldsymbol{S}_{\mathrm{RA},i} \circ \boldsymbol{V} = \boldsymbol{S}_{\mathrm{RA},i} \circ \boldsymbol{S}_{1,i}\dot{\theta}_{1,i} \tag{14}$$

From Eq. (14), the Jacobian matrix J_{a} is obtained as

$$J_{\mathrm{a}} = \begin{bmatrix} \boldsymbol{s}_{\mathrm{RAf},1}^{\mathrm{T}} / (\boldsymbol{S}_{\mathrm{RA},1} \circ \boldsymbol{S}_{1,1}) \\ \boldsymbol{s}_{\mathrm{RAf},2}^{\mathrm{T}} / (\boldsymbol{S}_{\mathrm{RA},2} \circ \boldsymbol{S}_{1,2}) \\ \boldsymbol{s}_{\mathrm{RAf},3}^{\mathrm{T}} / (\boldsymbol{S}_{\mathrm{RA},3} \circ \boldsymbol{S}_{1,3}) \end{bmatrix}. \tag{15}$$

E. Identification of Singular Surfaces and Utility Workspace

As described in [21] and other literatures, singular points exist on surfaces inside the reachable workspace. If the signs of determinant of Jacobian matrix J are different between two separate points, there must be a point to be $\det J = 0$: a singular point. Based on this idea, singularity surfaces considering constraint and actuation singularities are obtained as follows.

(1) Define lattice points in the XYZ space by equally dividing its space.

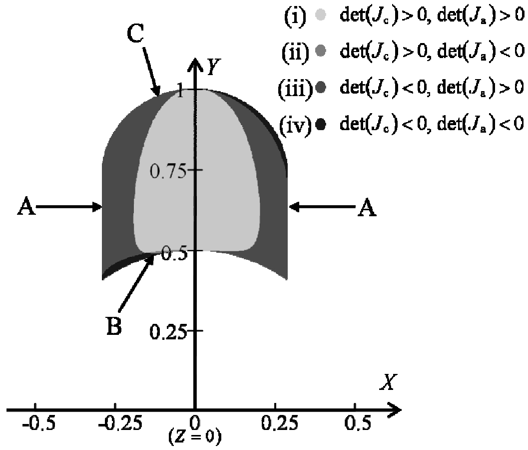

Figure 3. Combination of signs of matrices J_c and J_a in the reachable workspace (Z=0) ($r_p = r_b = 1$, $a_{12} = a_{23} = a_{34} = a_{45} = 0.25$)

(2) For all cases when each lattice point is given as the position of the platform, inverse displacement analysis is done.
(3) When real solution is obtained in (2), Jacobian matrices J_a and J_c are calculated. The signs of these matrices are then obtained. All the points where inverse displacement solution exists are classified into four sets by the combination of the signs of J_a and J_c.
(4) A singularity surface can be identified between two sets of points obtained in (3).
(5) Because one set of points may be distributed to two or more areas, utility workspace should be identified considering the cosecutiveness of points in one set.

Figure 3 shows a numerical example of distribution of the combination of signs of the Jacobian matrices for $r_b = r_p = 1, a_{12} = a_{23} = a_{34} = a_{45} = 0.25$. In Fig. 3, one set of points with the same signs combination is painted by a same density. From this result, we can identify singularity surfaces as the boundary between areas of different densities (i)-(iv). However, utility workspace can not be evaluated from this result. We need to develop an algorithm to check the consecutiveness of points in one region with the same combination of signs.

IV. Computational Algorithm of Utility Workspace

In the previous section, the reachable workspace of a 3-5R parallel mechanism was divided into four regions according to the combination of signs of determinants of Jacobian matrices J_a and J_c. However, as described, such a divided region may exist separately. So, utility workspace, from any point to any other points of which a mechanism can move without suffering from singularity and workspace boundary, should be identified considering the consecutiveness of points in one region. In this section, a computational algorithm to identify a utility workspace of a mechanism checking the consecutiveness of points is proposed.

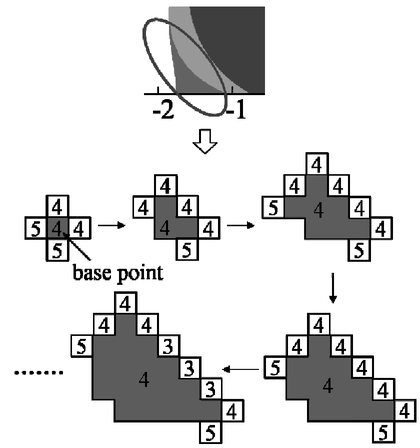

Figure 4. A visual explanation of the steps (4) and (5) to compute the utility workspace for planar case

The proposed algorithm is summarized as follows. Here, this algorithm is based on the calculation result mentioned in the previous section.
(1) Label all points inside the reachable workspace according to the combination of signs of determinants of the Jacobian matrices J_a and J_c.
(2) Choose one of the areas, at every point in which the label is the same, and which has labeled points. If there is no area, go to the step (7).
(3) Choose one point inside this area. This point is called a "base point". If there is no point, go to the step (2).
(4) Check the label of all the adjacent points of the base point. Obtain an initial area by combining all points around the base point, which have the same label, with the base point. This area is called "sub-workspace".
(5) Check the label of all adjacent points of the points that were combined with the initial sub-workspace in (4), and sub-workspace is updated according to the label following the same technique in (4). Repeat this step until the sub-workspace is not updated.
(6) The sub-workspace is considered as a closed area where the mechanism can move consecutively, and is registered. Delete all points which belong to this sub-workspace from the area, and go to the step (3).
(7) Determine the utility workspace as the area having the maximum volume among the registered sub-workspaces in (6). Here, though the workspace volume is used as the evaluation index, shape of the area and other measures can be used.

Operations in the steps (4) and (5) for a planar case are visualized in Fig.4. For spatial case, this algorithm can be applied.

V. Design of 3-5R Translational Parallel Mechanism with Consideration of Utility Workspace

A. *Enlargement of Reachable Workspace of 3-* $\dot{R}R\overline{RR}\dot{R}$ *Mechanism*

First, we investigated the workspace boundaries shown in Fig. 3 in order to enlarge the reachable workspace relative to

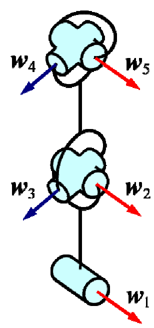

Figure 5. RUU-type connecting chain

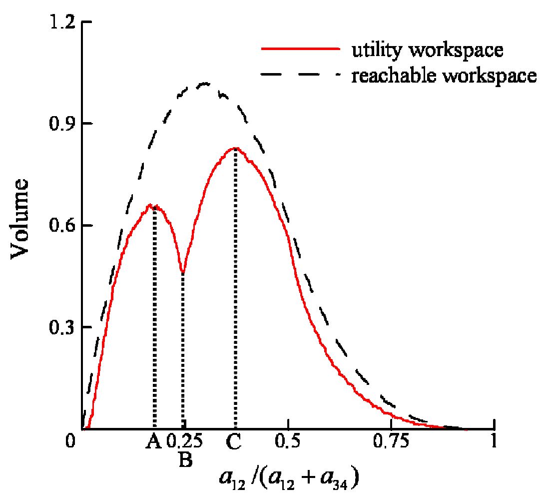

Figure 6. Link length ratio vs. volume of the utility workspace of 3-RUU parallel mechanism

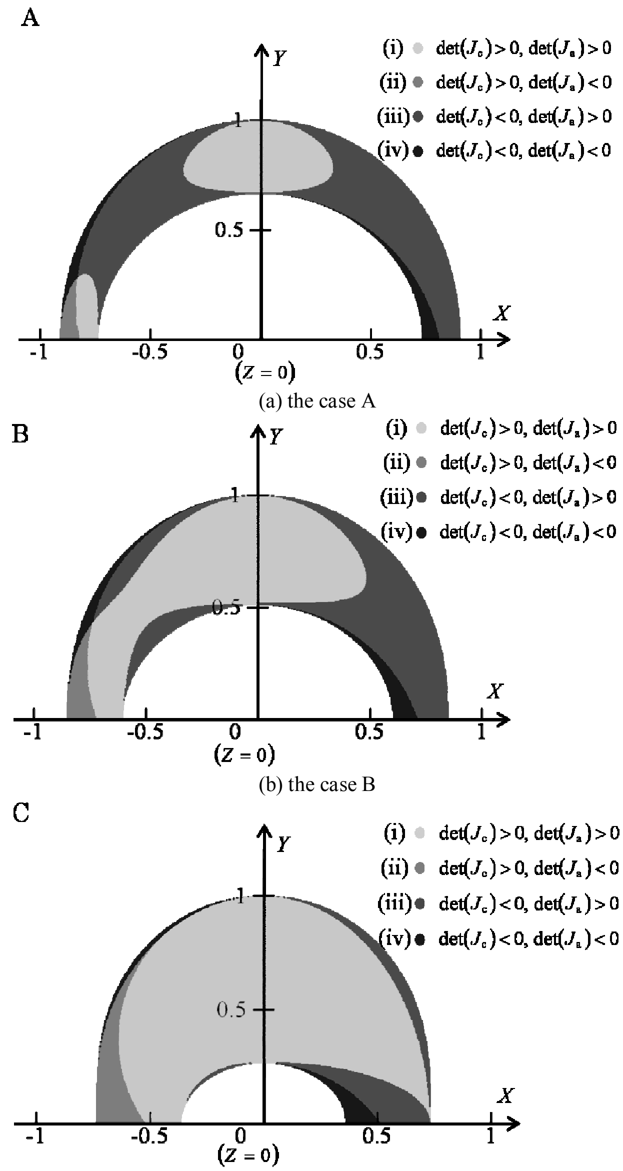

(a) the case A

(b) the case B

(c) the case C

Figure 7. Distributions of of the signs of $\det J_c$ and $\det J_a$ of 3-RUU translational parallel mechanism

the mechanism size. In Fig.3, three boundaries A, B and C are shown. Since the boundary C is caused by the limitation of total link length, enlargement of the boundary C results in expansion of the mechanism size. Then, we do not discuss about the boundary C. In what follows, enlargement of boundaries A and B is discussed.

We found from numerical calculations that the boundary A depends on the length a_{34}. In order to enlarge this boundary, it is necessary to lengthen a_{34}. On the other hand, we found that the boundary B is dependent on the difference between the link length a_{12} and the distance of joints 2 and 5. Through simulations, we found that a mechanism of $a_{23}=a_{45}=0$ can have a large reachable workspace. This corresponds to the 3-RUU mechanism as a special case of 3- $\dot{R}\dot{R}\overline{RR}\dot{R}$ translational parallel mechanism. An RUU chain is shown in Fig. 5.

B. Kinematic Design of 3-RUU Parallel Mechanism With Consideration of the Utility Workspace

Figure 6 shows the relationship between the link length ratio $a_{12}/(a_{12}+a_{34})$ ($a_{12}+a_{34}=1$) and the volume of the utility workspace of 3-RUU parallel mechanism. It is know from this figure that there are three peak points A($a_{12}/(a_{12}+a_{34})=0.17$), B($a_{12}/(a_{12}+a_{34})=0.245$) and C($a_{12}/(a_{12}+a_{34})=0.37$). Distributions of the combination of signs of determinants $\det J_a$ and $\det J_c$ are shown in Fig. 7 for these three cases. The case A leads to the maximization of the area of the sub-workspace (iii). The case C leads to the maximization of the area of the sub-workspace (i). In the case B, the sub-workspaces (i) and (iii) have the same volume. It is known from Fig. 6 that the kinematic constants for these two cases A and C are different from that leading to the maximization of the reachable workspace. When the kinematic constants are chosen as the case C, that is the case with the largest utility workspace, it is known from Fig. 7(c) that one of the four sub-workspaces, (i), occupies most of the reachable workspace, and this results in the maximization of the utility

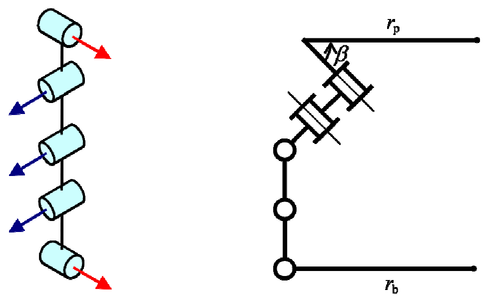

(a) $\dot{R}\overline{RRR}\dot{R}$ -type (b) $\dot{R}\dot{R}\dot{R}\overline{RR}$ -type

Figure 8. Two connecting chains applicable to 3-5R translational parallel mechanism

workspace. Therefore, in the design of practical parallel mechanism having a large utility workspace, it is important to evaluate the volume of the utility workspace. The volume of the utility workspace for the case C is 0.83. Its NVI (normalized volume index) [18] is 0.39. From this value, it is known that the 3-RUU translational parallel mechanism having kinematic constants corresponding to the case C has a large utility workspace relative to the size of the mechanism.

C. Utility Workspace of 3-5R Parallel Mechanism Having Other Connecting Chains

Connecting chains applicable to 3-5R translational parallel mechanism other than the $\dot{R}\dot{R}\overline{RR}\dot{R}$ chain are shown in Fig. 8.

First, $\dot{R}\bar{R}\bar{R}\bar{R}\dot{R}$ type connecting chain is investigated. As is described in [4], the $\dot{R}\bar{R}\bar{R}\bar{R}\dot{R}$ type connecting chain is better than the $\dot{R}\dot{R}\overline{RR}\dot{R}$ type when the volume of the reachable workspace is considered. However, we found that 3-$\dot{R}\bar{R}\bar{R}\bar{R}\dot{R}$ translational parallel mechanism, in which the first revolute joints on the base are used as active joints, becomes singular (actuation singularity) in the *XY* plane. Therefore, the $\dot{R}\bar{R}\bar{R}\bar{R}\dot{R}$ type connecting chain is not useful as far as the actuators are located on the base link.

Next, we investigate the $\dot{R}\dot{R}\dot{R}\overline{RR}$ type connecting chain. When this type of connecting chain is used, the condition for constraint singularity is independent of the position of the platform. Therefore, it is possible to eliminate the constraint singularity by an appropriate kinematic design. This can be done by determining the angle β with consideration of the value of $\det J_c$. We investigated kinematic constants including β of this connecting chain evaluating the volume of the utility workspace. As an example, a distribution of the signs of $\det J_a$ is shown in Fig. 9, when kinematic constants shown in Table I are used. To determine these kinematic constants, we firstly investigated enlargement of reachable workspace. This resulted in $\dot{R}\dot{R}U\overline{R}$ connecting chain. Then, we optimized its kinematic constants taking the volume of the utility workspace into consideration. This result is summarized in the table.

It is known that constraint singularity doesn't exist in Fig.9. The utility workspace corresponds to the sub-workspace (i). Its

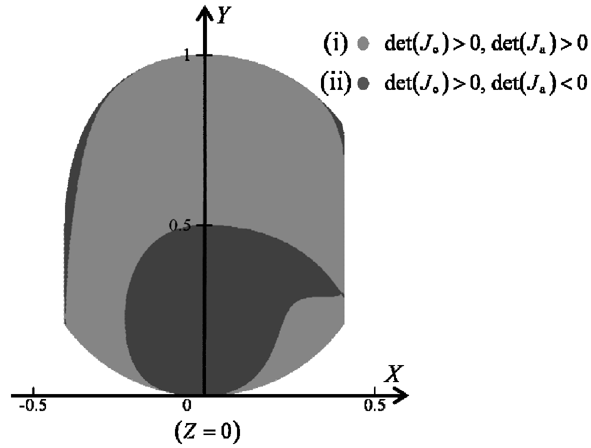

Figure 9. Distribution of the signs of $\det J_c$ and $\det J_a$ of a 3-$\dot{R}\dot{R}U\overline{R}$ translational parallel mechanism

TABLE I. KINEMATIC CONSTANTS OF 3-$\dot{R}\dot{R}U\overline{R}$ MECHANISM ($\gamma_1 = 0^\circ$, $\gamma_2 = 120^\circ$, $\gamma_3 = 240^\circ$, $r_p = r_b = 1$, $\beta = 45^\circ$)

j	a_{jk}	d_j
1	0.25	0
2	0.25	0
3	0	0
4	$\sqrt{2}/4$	$\sqrt{2}/4$

NVI is calculated as 0.13. From the view point of the utility workspace, the RUU-type connecting chain is considered better for translational parallel mechanism.

D. Prototype of 3-RUU Translational Parallel Mechanism With a Large Utility Workspace

Based on the results obtained in this section, we designed and built a prototype shown in Fig. 10. We conducted experiments to investigate the workspace of the prototype experimentally. As a result, the prototype achieved a stroke of 420mm in the *X*-direction while the maximum stroke in this direction is theoretically 490mm. It was also observed through experiments that orientation of the platform rapidly changed as it closed to the singular point. This will be investigated by sensitivity analysis as described in [25][26].

VI. CONCLUSIONS

In the present paper, we discussed about a kinamatic design of 3-5R translational parallel mechanism with a large utility workspace. We defined the utility workspace as a closed area, from any point to other points in which the mechanism can move without suffering from singularity and workspace boundary. A computational algorithm of the volume of the utility workspace was proposed. We obtained a 3-RUU translational parallel mechanism with a large utility workspace.

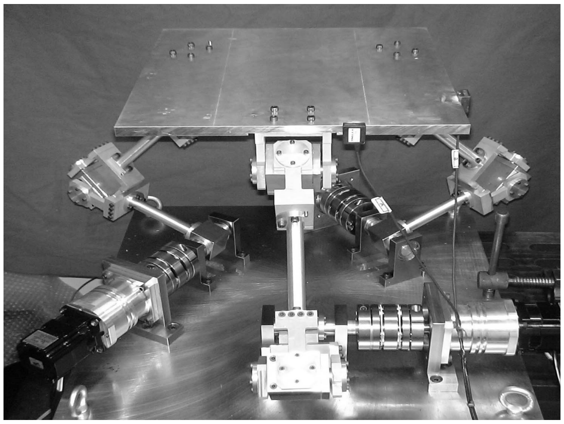

Figure 10. Prototype 3-RUU translational parallel mechanism
($r_p = r_b = 150$mm, $a_{12} = 205$mm, $a_{34} = 260$mm)

Acknowledgment

This work was supported in part by a Grant-in-Aid for Scientific Research from the Ministry of Education, Culture, Sports, Science and Technology (19560136).

References

[1] S. A. Joshi and L. W. Tsai, "Jacobian analysis of limited-dof parallel manipulators", Journal of Mechanical Design, Transactions of the ASME, v 124, n 2, June, pp. 254-258, 2002.

[2] S. Huda and Y. Takeda, "Mobility and workspace of a 3-5R translational parallel mechanism", Proceedings of 2006 ASME International Design Engineering Technical Conferences and Computers and Information In Engineering Conference, DETC2006, 2006.

[3] D. Kim and W. K. Chung, "Kinematic condition analysis of three-dof pure translational parallel manipulators", Journal of Mechanical Design, Transactions of the ASME, v 125, n 2, pp. 323-331, 2003.

[4] J. Yu, S. Bi, and T. Zhao, "Type synthesis of three-dof translational parallel mechanisms", Proceedings of the ASME Design Engineering Technical Conference, v 2 B, pp. 1107-1115, 2003.

[5] X. Kong and C. M. Gosselin, "Type synthesis of 3-dof translational parallel manipulators based on screw theory", Journal of Mechanical Design, Transactions of the ASME, v 126, n 1, January, pp. 83-92, 2004.

[6] S. A. Joshi and L. W. Tsai, "A comparison study of two 3-DOF parallel manipulators: One with three and the other with four supporting legs", Proceedings IEEE International Conference on Robotics and Automation, v 4, pp. 3690-3697, 2002.

[7] L. Romdhane, Z. Affi, and M. Fayet, "Design and singularity analysis of a 3-translational-DOF in-parallel manipulator", Journal of Mechanical Design, Transactions of the ASME, v 124, n 3, September, p 419-426, 2002.

[8] R. Di Gregorio, "Kinematics of the translational 3-URC mechanism", Journal of Mechanical Design, Transactions of the ASME, v 126, n 6, November, pp. 1113-1117, 2004.

[9] M. Carricato and V. Parenti-Castelli, "A family of 3-dof translational parallel manipulators", Proceedings of the ASME Design Engineering Technical Conference and Computers and Information in Engineering Conference. v 2, pp. 259-266, 2001.

[10] R. Di Gregorio and V. Parenti-Castelli, "Mobility analysis of the 3-UPU parallel mechanism assembled for a pure translational motion", IEEE/ASME International Conference on Advanced Intelligent Mechatronics, AIM, pp. 520-525, 1999.

[11] D. Chablat and P. Wenger, "Architecture optimization of a 3-DOF translational parallel mechanism for machining applications, the orthoglide", IEEE Transactions on Robotics and Automation, v 19, n 3, June, pp. 403-410 , 2003.

[12] M. Badescu, J. Morman, and C. Mavroidis, "Workspace optimization of 3-UPU parallel platforms with joint constraints", Proceedings IEEE International Conference on Robotics and Automation, v 4, pp. 3678-3683, 2002.

[13] Y. Li and Q. Xu, "A new approach to the architecture optimization of a general 3-PUU translational parallel manipulator", Journal of Intelligent and Robotic Systems: Theory and Applications, v 46, n 1, pp. 59-72, 2006.

[14] L. W. Tsai and S. Joshi, "Comparison study of architectures of four 3 degree-of-freedom translational parallel manipulators", Proceedings IEEE International Conference on Robotics and Automation, v 2, pp. 1283-1288, 2001.

[15] Y. Li and Q. Xu, "Design and development of a medical parallel robot for cardiopulmonary resuscitation", IEEE/ASME Transactions on Mechatronics, v 12, n 3, June, Advanced Integrated Mechatronics, pp. 265-273, 2007.

[16] G. Wu, J. Li, R. Fei, X. Wang, and D. Liu, "Analysis and design of a novel micro-dissection manipulator based on ultrasonic vibration", Proceedings IEEE International Conference on Robotics and Automation, v 2005, pp. 466-471, 2005.

[17] T. Tanikawa, M. Ukiana, K. Morita, Y. Koseki, K. Fujii, and T. Arai, "Design of 3DOF parallel mechanism with thin plate for micro finger module in micro manipulation", IEEE International Conference on Intelligent Robots and Systems, v 2, p 1778-1783, 2002.

[18] D. C. H. Yang and Y. Y. Lin, "Pantograph mechanism as a non-traditional manipulator structure", Mechanism and Machine Theory, v 20, n 2, pp. 115-122, 1985.

[19] Y. Wang and C. M. Gosselin, "On the design of a 3-PRRR spatial parallel compliant mechanism", Proceedings of the ASME Design Engineering Technical Conference, v 2 A, pp. 387-395, 2004.

[20] H. S. Kim, and L. W. Tsai, "Design optimization of a Cartesian parallel manipulator", Journal of Mechanical Design, Transactions of the ASME, v 125, n 1, March, pp. 43-51, 2003.

[21] Y. Takeda and H. Funabashi, "Kinematic and static characteristics of in-parallel actuated manipulators at singular points and in their neighborhood", JSME International Journal, Series C, v 39, n 1, pp. 85-93, 1996.

[22] D. Zlatanov, I. Bonev and C. M. Gosselin, "Constraint singularities of parallel mechanisms", Proceegings of IEEE International Conference on Robotics and Automation, pp. 496-502, 2002.

[23] A. Wolf, M. Shoham and F. C. Park, "Investigation of singularities and self-motions of the 3-UPU robot", Advances in Robot Kinematics, pp. 165-174, 2002.

[24] S. Huda and Y. Takeda, "Kinematic analysis and synthesis of a 3-URU pure rotational parallel mechanism with respect to singularity and workspace", *Journal of Advanced Mechanical Design, System and Manufacturing*, Vol. 1, No. 1, pp.81-92, 2007.

[25] C. H. Han, J. W. Kim, J. W. Kim, and F. C. Park, "Kinematic sensitivity analysis of the 3-UPU parallel mechanism", Mechanism and Machine Theory, v 37, n 8, August, pp 787-798, 2002.

[26] S. Huda and Y. Takeda, "Kinematic design of 3-URU pure rotational parallel mechanism with consideration of the uncompensated error", Proceedings of the 13th Robotics Symposia, pp.504-509, 2008.